

A portable instrument for high-speed brain function imaging: fEITER

Hugh McCann *Senior Member, IEEE*, S. Talha Ahsan, John L. Davidson, Rebecca L. Robinson,
Paul Wright, and Chris J. D. Pomfrett

Abstract— Electrical Impedance Tomography (EIT) can resolve dynamic physiological information deep within human subjects [1], but its sensitivity is challenged in the case of imaging the head [2]. Here, we report a new system called fEITER that has been designed and built to enable functional imaging of the human brain using EIT via scalp-mounted electrodes, integrated with stimulation of evoked responses. Using Field-Programmable Gate Array (FPGA) technology, it provides excellent flexibility in terms of current-pattern excitation and signal processing. The instrument operates at 100 frames/second (fps) with noise of 1 μV on the rms voltage measurements. Clinical trials have been authorized by the UK MHRA and example data from human subjects are presented.

I. INTRODUCTION

ELECTRICAL Impedance Tomography has become well established for imaging in both medicine and process engineering, exploiting its portability and speed. Its applications include lung function imaging [1] and multi-phase flow characterization [3]. There has been considerable interest in its capability to provide dynamic images of human brain function [2, 4-6], via conductivity changes due to:

1. electrical effects in regions of high synaptic density [7],
2. the haemodynamic consequences of brain function [8], or
3. some combination thereof.

Process 1 above extends over a period of around 500 ms in response to a short stimulus, but includes more rapid phases of tens of ms or less, whereas process 2 occurs over several seconds. In [4], a target measurement precision of about 10^{-4} of the measured voltages is identified, to enable imaging of a 4% change in conductivity in the visual cortex, although those calculations are pessimistic in that they used a significantly lower value of skull conductivity, σ_s , than the current best measurements of around 0.050 S/m [9].

Manuscript received April 14, 2011. This work was supported in part by the Wellcome Trust under Grant 077724/Z/05, and by the UK EPSRC through a doctoral training grant to RLR.

H. McCann (corresponding author, +44 161-306-4791; e-mail: h.mccann@manchester.ac.uk), J. L. Davidson and P. Wright are with the School of Electrical and Electronic Engineering, University of Manchester, Manchester, UK.

S. T. Ahsan and R. L. Robinson were with the School of Electrical and Electronic Engineering, University of Manchester, Manchester, UK, and are now with, respectively, Bahria University, Karachi, Pakistan, and the University of Liverpool, Liverpool, UK.

C. J. D. Pomfrett was with the School of Biomedicine, University of Manchester, and the Department of Anaesthesia, Manchester Royal Infirmary, Manchester, UK and is now with the National Institute for Clinical Excellence, Manchester, UK.

We report here a new design of medical EIT system that achieves high-speed imaging (100 fps) whilst also achieving excellent low-noise performance that approaches the target precision identified in [4]. The implementation and construction of the system is described, and its performance is evaluated in both laboratory and human tests. In the latter case, the above combination of measurement/imaging speed and precision has enabled novel observations of a number of phenomena, particularly the multi-site measurement of rheoencephalography (REG) [10] and the response of various brain regions to extreme auditory stimulation.

II. SYSTEM DESCRIPTION

A. Hardware

The system (Fig. 1) includes three Type BF applied parts, *viz.* the EIT sub-system (with its electrodes and connecting leads), and visual and auditory stimulus sub-systems. It is housed in two sub-assemblies: a *Base Unit* and a *Headbox*. The base unit provides power to all sub-systems, incorporates the stimulus sequencing sub-system (CED micro1401), and acquires and formats data for export to the system laptop computer that is also provided for user communication with the hardware and for the generation of stimulus sequences using *Signal* software (CED). The auditory stimulus sub-system consists of a pair of inner-ear headphones, or optionally large-format TDH headphones (Telephonics), driven from the CED micro1401, via a separation device as a means of patient protection (MOPP). The visual (flash) stimulus is delivered by two 5×4 arrays

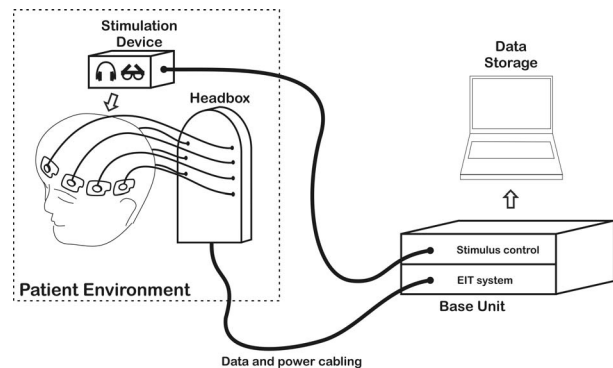


Fig. 1: Schematic diagram of the fEITER system.

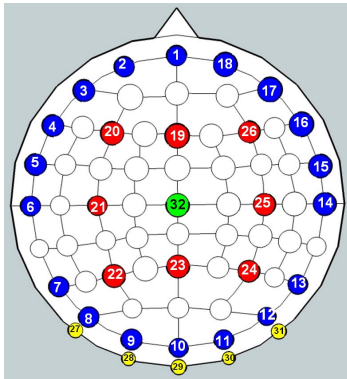


Fig. 2: The 32 scalp-mounted Covidien Zipprep™ electrodes arranged on a sub-set of the EEG 10-20 array locations. The subject's nose is at the top and the view is from the crown of the head.

(7.5 mm pitch) of RGB LEDs with associated diffusers, mounted approx. 13 mm from the subject's eyes, within a pair of goggles. The resulting angular subtense is intended to ensure stimulation of the full visual field, irrespective of the pre-stimulus fixation state of the eye. Two-MOPP patient protection is provided by the construction of the goggles. Stimulus event markers are encoded in the system output data format with a resolution of 0.5 ms.

Using a local CPLD (Xilinx XC95144), the base unit carries out serial-to-parallel (8 bits) conversion of incoming data from the headbox, and the data are read out at 500 kS/s by a National Instruments USB DAQCard-6221 controlled using LabVIEW. The base unit provides the required two-MOPP separation between the patient circuit and live parts, including not only secondary circuits (3 kV rms) but also the mains part (4 kV rms).

The majority of the EIT sub-system hardware and firmware functionality lies within the headbox, which contains a Xilinx Virtex-4 SX35 FPGA and unique circuits for current sources, electrode interfaces and voltage measurements. All circuits are mounted on an 8-layer PCB that provides shielding between digital and analogue elements. Zipprep™ electrodes (Covidien Inc.) were found [11] to present relatively low impedance (typically 1.5 k Ω) to the 10 kHz sinusoidal current excitation (1 mA pk-to-pk) and were used throughout. The headbox connects to 32 scalp electrodes (plus one reference), arranged as shown in Figure 2, by snap-on touch-proof (non-shielded) cables (Integral Process S.A.). The headbox includes circuitry that renders the system robust against electro-surgery, although measurement performance is compromised during these procedures. Based on an enhanced Howland circuit, the current-drive circuits show excellent low-noise properties [12]. Current-sense resistors in the headbox, in conjunction with the FPGA, measure the applied current and check compliance with safety limits (IEC 60601-1:2005).

B. Firmware

The FPGA performs Direct Digital Synthesis (DDS) of the current excitation waveform, and controls CMOS switches to provide current excitation between any desired pair of electrodes; in the work reported here, a fixed set of

20 near-diametric current-patterns (CPs) were used, geometrically optimized for sensitivity to the visual cortex. During each 500 μ s (5 cycle) CP, simultaneous voltage measurements are made between all adjacent headbox inputs (except those involving the current excitation electrodes), sampled at 500 kS/s using 16-bit ADCs. Phase-sensitive demodulation (PSD) is implemented on the FPGA to determine the voltage amplitude that is synchronous with the current excitation, and their relative phase, from 4 cycles of sampled voltages (the first current cycle after CP switching is not used), yielding an effective measurement bandwidth of 5kHz. The above measurement protocol yields 546 EIT voltage measurements per frame. It should be noted that, in order to eliminate any scope for misunderstanding in the remainder of this paper, we discuss the rms voltage measurement, in contrast to recent conference presentations (e.g. [13]) where we have reported peak-to-peak voltage measurement.

III. SYSTEM PERFORMANCE

A. Phantom Studies

Objective performance measurement of EIT instruments on human subjects is hampered by several factors, including the presence of various physiological signals, most obviously REG. Studies on phantoms are therefore attractive but it should be recognised that coupled noise and interference levels will depend markedly on the geometric form of the phantom. We have used precision resistor-based wheel phantoms for measurements of intrinsic instrument performance, and saline-filled 'head-like' tanks for measurements intended to include a representative contribution from coupled interference. We define two measurement timescales of interest: 1) short term - a 500 ms (50 frame) epoch, to represent a single functional response event, and 2) long term - a 1-minute (6000 frame) epoch, typical of a single experiment with a given stimulus pattern. Table I summarises the noise performance of the fEITER measurement system for both timescales and phantom types. Although the individual voltage signals in an EIT experiment depend on both the characteristics of the measurement subject and the arrangement of electrodes, the observed repeatability on head-like phantoms indicates a

TABLE I
NOISE PERFORMANCE MEASURES

Phantom type / Timescale	Short term	Long term
Resistor wheel ^a	1	1
Head-like saline tank ^b	3.1 – 3.4 ^c	3.8 – 4.2 ^c

All noise values are expressed as standard deviation in measured voltage (μ V) and are influenced by the quantisation noise floor (1.36 μ V) of the 16-bit data representation used.

^a0.1% 10ppm/K resistor network, giving inter-electrode drive impedance of 338 - 418 Ω , mounted directly onto headbox connectors.

^bNominal conductivity 500 μ S/cm connected via 60 cm unshielded leads.

^cEnvironment dependent; ranges shown typify our experience in both laboratory and hospital environments.

potential SNR of over 90 dB for a full scale (108 mV rms) input signal). Note that the SD values in the resistor phantom case slightly underestimate the true population SD, due to the quantisation of the 16-bit data representation. Although adequate under normal circumstances, this does have a discernible effect at the reduced levels of signal variation possible in phantom tests.

B. Human Data

Human tests are being conducted at Manchester Royal Infirmary, notified to the UK MHRA. Figure 3 illustrates the stability of the raw voltage measurements obtained from human tests on a short-term basis, under non-stimulus conditions. The measured data broadly agree with forward calculations performed by EIDORS 3D [14], using a 7-tissue head model [15] with a total of 53,336 tetrahedral elements, and with σ_s set at 0.05 S/m, although it is clear that the model calculation clearly could be optimised further.

The individual voltage measurements on human subjects always contain a cardiac-related waveform, as shown in

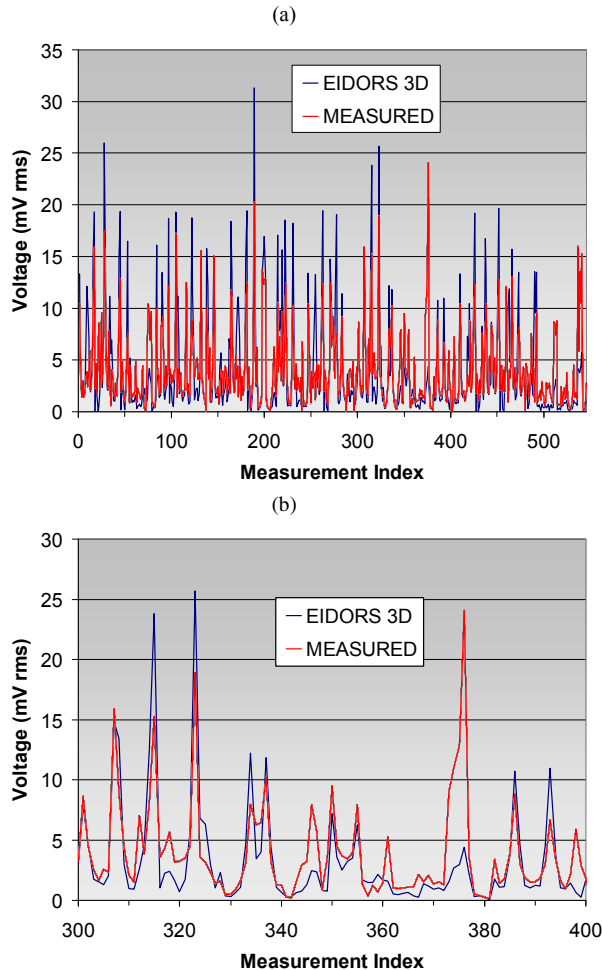


Fig. 3: An overlay of 50 frames of measured voltages on a human subject, compared with forward calculations (EIDORS), (a) whole frames of 546 measurements, (b) measurements 300 – 400.

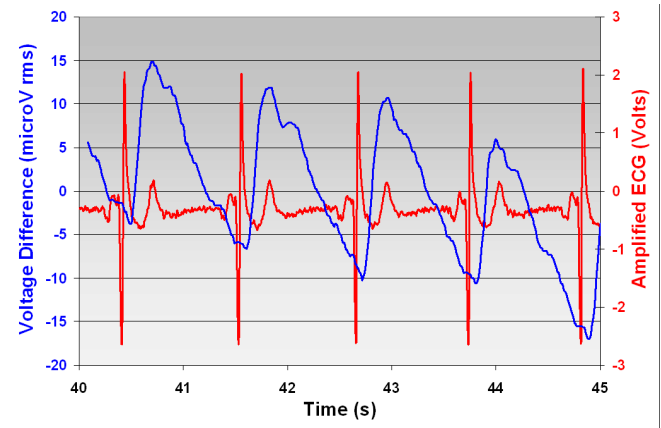


Fig. 4: Time variation (in blue) of the voltage measurement for CP 5-15 and voltage measurement 19-20, relative to the 1-minute mean value; it is shown here as a 10-sample moving average. The red trace shows the simultaneous electrocardiogram (ECG).

Figure 4 for measurement 5-15-19-20. The positive peak in the EIT waveform occurs typically 200 ms after the ‘R’ wave (highest positive peak) in the ECG, which is associated with ventricular action. This aspect of the fEITER data is attributed to the rheoencephalographic (REG) signal which has been reviewed recently by Bodo [10]. We find that the peak-to-peak magnitude of the REG-related waveform in the fEITER data depends on scalp location and varies over 5 - 20 μV , i.e. typically larger than system noise effects.

IV. STIMULUS RESPONSE

We report here an example from preliminary tests on two subjects, using a gross auditory stimulus, *viz.* release of a party-popper a few metres from the subjects, who were blindfolded. (Although optimized for visual cortex sensitivity, the 20 CPs include at least 6 with left-right geometry and thus sensitive to the auditory cortices.) Subject A was informed only that there would be a surprise stimulus, whereas subject B had heard it before the experiment. We expect these conditions to evoke the auditory startle reflex (ASR) which is a measure of the brainstem response [16]. Subject A has a severe hearing impairment in the left ear (55 dB down), and was exposed to the stimulus only three times. Subject B was exposed to 8 party-popper events over a period of 42 minutes.

Transient fEITER voltage changes for both subjects showed some effects in the order of 300 μV rms. Whereas the fEITER responses of Subject B were broadly left-right (L-R) symmetric, the responses of Subject A were extremely L-R asymmetric, with some voltage data changes measured on the left (e.g. 6-14-21-22) showing orders of magnitude greater response than the equivalent one on the right (e.g. 6-14-24-25). (This difference between the two subjects was confirmed in tests with much more carefully controlled auditory stimuli that elicited substantially smaller responses, of order 20 μV .) These observations are consistent with the subjects’ relative hearing ability and with contralateral neural processing. The observed fEITER responses

measured near the auditory cortices for both subjects show features resembling, in latency and in relative form, the well-established P1-N1-P2 complex observed in EEG monitoring of auditory evoked potentials [17]. The measured EIT voltage responses of Subject B to gross auditory stimulus show clear evidence of habituation; at symmetric locations near left and right auditory cortices they contain short-term components (< 1 sec, ~ 20 μ V) and long-term components (several sec, ~ 50 μ V), which are characteristic of these tests.

The large EIT voltage changes measured (with respect to an initial reference interval) in these gross auditory tests, allow reconstruction of images of conductivity change due to stimulus, even disregarding the effects of the REG. Image reconstruction was carried out for each frame using an SVD algorithm, and using a sub-set region of 24,465 elements of the head model, comprising of the grey and white matter and CSF. An example image is shown in Figure 5, where there appears to be substantial activation in the cerebellum, linked to brain stem activity. Image reconstruction was carried out off-line, although it can be anticipated that, eventually, some degree of image reconstruction will be carried out on-line.

V. DISCUSSION AND CONCLUSIONS

The new 32-electrode medical EIT system reported here has a relatively high frame rate, at 100 fps, and is fully integrated with a flexible stimulus evoking system. It exhibits very good noise performance. For example, it is broadly comparable in that respect with the best of the three systems discussed by Fabrizi et al. [18], who carried out phantom tests of a similar nature, but with much reduced measurement bandwidth compared with our system. The new fEITER system certainly appears to enjoy a unique *combination* of frame rate and noise performance. This configuration has revealed the importance of the REG-related component of the EIT signal when measured on the human head. The utility of fEITER for brain function imaging continues to be the subject of on-going clinical and research investigations in Manchester [19]. In this paper, we have presented examples of data obtained that may plausibly be due to neural processing. However, firm conclusions on this point await analysis of the statistically large sample of subjects that is being amassed in the clinical investigation.

REFERENCES

- [1] G. Hahn et al., "Imaging pathologic pulmonary air and fluid accumulation by functional and absolute EIT", *Physiol. Meas.*, vol. 27, pp. S187-S198, 2006.
- [2] C. M. Towers, H. McCann, M. Wang, P. C. Beatty, C. J. D. Pomfrett, and M. S. Beck, "3D simulation of EIT for monitoring impedance variations within the human head," *J. Physiol. Meas.*, vol. 21, pp. 119-124, 2000.
- [3] T. York, "Status of electrical tomography in industrial applications," *Journal of Electronic Imaging*, vol. 10, no. 3, pp. 608-619, 2001.

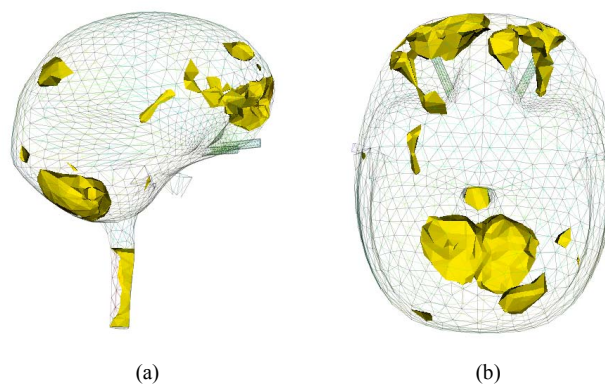


Fig. 5: Isosurfaces of 3D reconstructions of conductivity change at 800 ms after gross auditory stimulus: (a) elevation view; (b) plan view (subject A).

- [4] N. Polydorides, W. R. B. Lionheart, and H. McCann, "Krylov subspace iterative techniques : On the detection of brain activity with Electrical Impedance Tomography," *IEEE Trans. Med. Im.*, vol. 21, pp. 596-603, 2002.
- [5] A. T. Tidswell, A. Gibson, R. H. Bayford, and D. S. Holder, "Three-Dimensional Electrical Impedance Tomography of Human Brain Activity," *NeuroImage*, vol. 13, pp. 283-294, 2001.
- [6] H. McCann, N. Polydorides, J. C. Murrieta-Lee, G. Kou, P. Beatty and C. J. D. Pomfrett, "Sub-second functional imaging by Electrical Impedance Tomography", in 28th Annual International Conference EMBS, New York City, NY: IEEE, 2006, pp. 4269-4272.
- [7] K. A. Klivington, "Effects of pharmacological agents on subcortical resistance shifts," *Exp. Neurol.*, vol. 46, pp. 78-86, 1975.
- [8] N. K. Logothetis, "What we can do and what we cannot do with fMRI", *Nature*, vol. 453, pp. 869-878, 2008.
- [9] R. Hoekema et al., "Measurement of the Conductivity of Skull, Temporarily Removed During Epilepsy Surgery," *Brain Topogr.*, vol. 16, no. 1, pp. 29-38, 2003.
- [10] M. Bodo, "Studies in Rheoencephalography (REG)", *J. Electrical Bioimpedance*, vol. 1, pp. 18-40, 2010.
- [11] R. L. Robinson, P. Wright, J. L. Davidson, C. J. D. Pomfrett and H. McCann, "A Study of Composite Electrode-Tissue Impedance", in 30th Annual International Conference EMBS, Vancouver, BC, Canada: IEEE, 2008, pp. 1171-1174.
- [12] M. Rafiei-Naeini and H. McCann, "Low-noise current excitation sub-system for medical EIT", *Physiol. Meas.*, vol. 29, pp. S173-S184, 2008.
- [13] J.L. Davidson, P. Wright, S.T. Ahsan, R.L. Robinson, C.J.D. Pomfrett and H. McCann, "fEITER: A New EIT Instrument for Functional Brain Imaging", *J. Phys.: Conference Series*, vol. 224, 012025, 2010
- [14] N. Polydorides N and W.R.B. Lionheart, "A Matlab based toolkit for three-dimensional electrical impedance tomography: a contribution to the EIDORS project", *Meas. Sci. Technol.* vol. 13, pp. 1871-8, 2002.
- [15] D.S. Holder, private communication 2010.
- [16] M.J. Bakker et al., "Quantification of the auditory startle reflex in children", *Clin. Neurophysiology*, vol. 120, pp. 424-430, 2009.
- [17] B.A. Martin, K.L. Tremblay K L, and D.R. Stapells D R, , Principles of Cortical Auditory Evoked Potentials, pp. 482 – 507, in *Auditory Evoked Potentials, Basic Principles and Clinical Application*, (eds. Burkard R F, Eggermont J J, and Don M), Lippincott Williams and Wilkins, 2007.
- [18] L. Fabrizi, A. McEwan, E. Woo and D. S. Holder, "Analysis of resting npiise characteristics ofthree EIT systems in order to compare suitability for time difference imaging with scalp electrodes during epileptic seizures ", *Physiol. Meas.* vol. 28, pp. S217-S236, 2007.
- [19] A. Bryan, C.J.D Pomfrett, J.L. Davidson, B.J. Pollard, T. Quraishi, P. Wright, R.L. Robinson, S.T. Ahsan and H. McCann, "Functional electrical impedance tomography by evoked response: a new device for the study of human brain function during anaesthesia", *Proc. Anaesthetic Research Society*, in *British J. Anaesthesia* vol. 106, pp. 428–9, 2011